CHARACTERIZATION AND DISCRIMINATION OF PLANT FOSSILS BY ATR-FTIR, XRD AND CHEMOMETRIC METHODS

STELUȚA GOSAV[1], ANTOANETA ENE[1,]*, MAGDALENA AFLORI[2]

[1] *Dunarea de Jos* University of Galati, Faculty of Sciences and Environment, Department of Chemistry, Physics and Environment, 47 Domneasca St., 800008 Galati, Romania
*Corresponding author: aene@ugal.ro
[2] *Petru Poni* Institute of Macromolecular Chemistry of Romanian Academy, 41A Grigore Ghica Voda Alley, 700487 Iasi, Romania

Received February 19, 2018

Abstract. In this paper we have investigated some samples of fossil leaves and their related mineral matrices using *Attenuated Total Reflectance – Fourier transform infrared* (ATR-FTIR) spectroscopy, *X-ray diffraction* (XRD) and Cluster Analysis and Principal Component Analysis chemometric methods. By using ATR-FTIR technique, we have identified the presence of organic and inorganic chemical groups in the studied samples. The organic carbon, derived from the decomposition of plants, was identified in ATR-FTIR spectra of fossil leaf samples by the presence of two sharp absorption peaks at around 2926 and 2852 cm^{-1} which had a higher intensity than those of the mineral matrix. An improvement of the discrimination power between the biotic and abiotic materials by using ATR-FTIR spectra in combination with chemometrics was achieved. Also, the mineralogical and elemental composition of the samples obtained by XRD technique is discussed.

Key words: plant fossils, ATR-FTIR, XRD, chemometric methods.

1. INTRODUCTION

The fossil-bed natural reservation at Chiuzbaia, Maramureş County, north-west of Romania, studied in the last decades by Razvan Givulescu [1 and the references therein], deposits a great variety of fossils representing stored vegetal remains of a luxury forest dated before the appearance of the human on Earth, *i.e.*, Late Miocene Epoch (11.6 million to 5.3 million years ago). The richness of the fossil material and discovered species and genera makes the flora of Chiuzbaia be unique in the south-east part of Europe [1].

The geochemical characterization of parent rock and organic matter preserved in ancient sedimentary structures is highly relevant for the fossiliferous complexes worldwide. Many papers highlighted the importance of applying the *Fourier Transform Infra-Red* (FTIR) spectroscopy technique for the fast and accurate identification of organic and mineralogical components in coal [2], shale [3] and other sedimentary rocks [4, 5], as well as of ancient life forms and interpretation of biosignatures in early terrestrial rocks [5]. Information regarding the composition

of sedimentary rocks can be obtained using FTIR method, since organic matter and minerals present most of their characteristic vibration modes in the IR spectral region [5]. Also, IR spectroscopic characterization could be employed in palaeobotany, since the plant cuticle is commonly preserved in organic fossils, and it is the main component of certain organic deposits [5, 6]. In the last years, the *Attenuated Total Reflectance* (ATR) in conjunction with FTIR spectrometer has become a very used technique, especially for the nondestructive measurement of both transmittance and absorbance IR spectra of samples with little or no preparation [6–12]. Very useful for processing of infrared spectra are the multivariate statistical methods, *e.g. Cluster Analysis* (CA), *Principal Component Analysis* (PCA), etc. Their great advantage is the capability to extract from the IR spectra important spectral information necessary for qualitative/quantitative analysis [13, 14].

The aim of this paper was to investigate, from the spectroscopic and chemometric point of view, ten samples collected from fossiliferous sites at Chiuzbaia deposit, Romania, representing sedimentary rocks (class A) and fossil leaves (class B) incorporated in these rocks. The ATR-FTIR spectra of these samples supplied us important information regarding the organic and inorganic functional groups present in both types of samples (A and B). Also, we proposed to investigate the sensitivity of ATR-FTIR technique and of ATR-FTIR coupled with chemometric methods, regarding the power of discrimination of B samples from the A type. The mineralogical and elemental composition of the samples was obtained using *X-ray diffraction* (XRD) technique.

2. MATERIAL AND METHODS

2.1. SAMPLE PREPARATION

All ten samples were collected from sedimentary rocks existed in the fossil-bed reservation of Chiuzbaia, Romania. The first five samples, labeled S_{1F}, S_{2F}, S_{3F}, S_{4F} and S_{5F}, represent the fossil leaves belonging to the class A, and the next five – *i.e.*, S_1, S_2, S_3, S_4 and S_5 – are their sedimentary matrices from the class B (sediment samples) (Fig. 1). By a fine scraping of fossil material we obtained the necessary powder amount for analysis, which is in the milligram range.

2.2. ATR-FTIR SPECTRA AND COMPUTATIONAL DETAILS

ATR-FTIR spectra of samples were recorded in the range 4000–400 cm^{-1}, in absorbance mode, with the aid of a Bruker Tensor 27 FTIR spectrometer from INPOLDE research center at Dunarea de Jos University of Galati, Romania, using a diamond ATR accessory [8]. All spectra were collected as a mean of 32 scans,

at a resolution of 4 cm^{-1}, and a background spectrum was recorded before each individual analysis. Separation of the overlapping bands found into the complex 1300–850 cm^{-1} absorption band was obtained by deconvolution using OriginPro 2016 (version 9.3.226) software. Curve fitting was performed by setting the number of component bands found by second derivative analysis and Lorentzian profile.

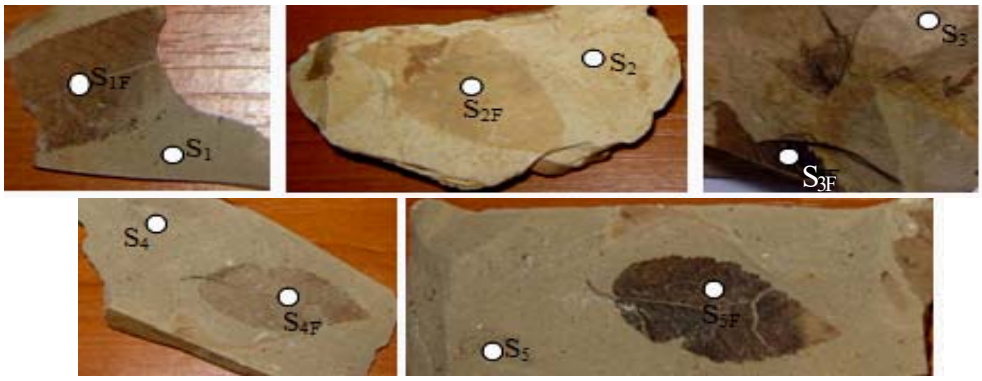

Fig. 1 – The investigated fossil plant leaves (S_{1F}–S_{5F}) and their sedimentary matrices (S_1–S_5).

In order to find the wavenumbers with the best discrimination power between the two classes, class B – the fossil leaves and class A – the mineral matrices, we computed the Fisher's weight, $W_i(B,A)$, using the following equation:

$$W_i(B,A) = \frac{[\overline{X}_i(B) - \overline{X}_i(A)]^2}{S_i^2(B) - S_i^2(A)} \quad (1)$$

where $\overline{X_i}(A)$ and $\overline{X_i}(B)$ are the means of variable X_i (absorption at the corresponding $\bar{\nu}_i$ wavenumber) for the samples of the A and B classes; $S_i(A)$ and $S_i(B)$ are the standard deviations of variable X_i in the case of samples of the A and B classes. Thus, from all variables (1866 absorptions for each spectrum), we retained only 234, which had the Fisher's weight greater than 2.2. These variables were auto-scaled and used as inputs for CA and PCA techniques, available from STATISTICA 12.5 software.

2.3. X-RAY DIFFRACTION SPECTRA

The mineralogical and elemental analyses of the samples were carried out using X-ray diffraction (D8 Advance, Bruker AXS) at "Petru Poni" Institute of Macromolecular Chemistry of Romanian Academy, Iasi, Romania. The X-rays were generated using a Cu-K_α source with an emission current of 36 mA and a voltage of 30 kV. Scans were collected over the 2θ = 10–60° range using a step size of 0.01 and a count time of 0.5 s/step. Semi-quantitative analysis was

performed with the EVA software from the DiffracPlus package (Bruker AXS) using the ICDD-PDF2 database, on the basis of the relative heights of the patterns.

3. RESULTS AND DISCUSSION

3.1. SPECTROSCOPIC ANALYSIS

In order to better visualize all the IR absorption peaks (Fig. 2), we performed a magnification of spectral regions specific to the stretching and bending vibrations of OH and CH_2 groups, as well as a deconvolution (Fig. 3) of the complex Si-O absorption band comprised between 850 and 1300 cm^{-1}.

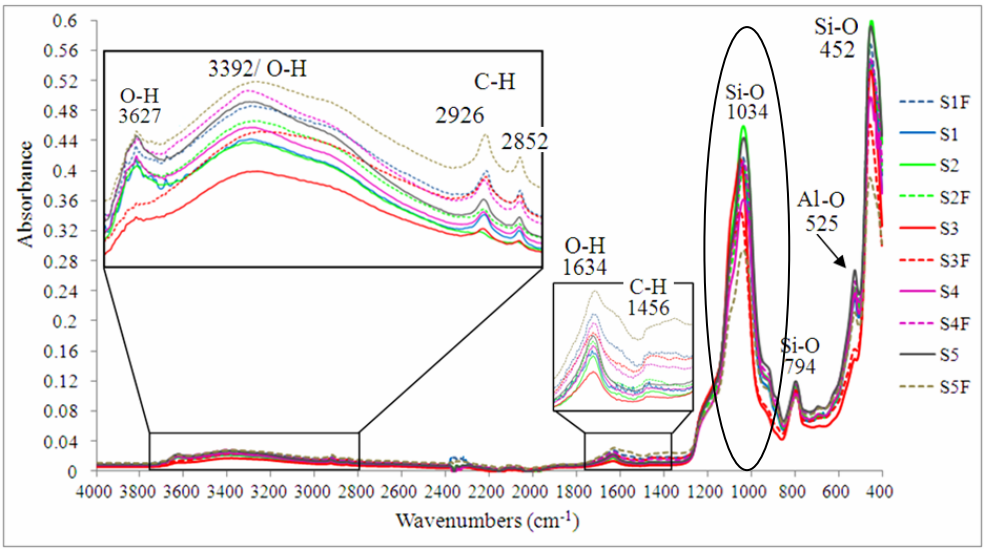

Fig. 2 – (Color online) ATR-FTIR spectra of all the samples – continuous line for S_{1-5} samples and dotted line for S_{1F-5F} samples.

Analyzing the ATR-FTIR spectra of all the studied samples (Fig. 2), we found their mineralogical composition by the identification of absorption bands attributed to the inorganic functional groups characteristic of quartz (SiO_2), kaolinite ($Al_2Si_2O_5(OH)_4$) and montmorillonite ($(Na,Ca)_{0.33}(Al,Mg)_2(Si_4O_{10})(OH)_2 \cdot nH_2O$) minerals. Thus, in the case of quartz, the characteristic IR absorption peaks appear at 1098 cm^{-1} (Fig. 3) and 794 cm^{-1} due to the stretching Si-O vibrations, and at 452 cm^{-1} attributed to the bending Si-O-Si vibrations [3]. Kaolinite and montmorillonite are two types of clay minerals formed by stacking structural layers namely, 1:1-type and 2:1-type of structural layers, respectively. In the former, the structural layer consists of stacked tetrahedral sheet (Si-O tetrahedrons) and

octahedral sheet (mainly Al-O octahedrons) while in the latter, the structural layer is composed of octahedral sheet sandwiched by two tetrahedral sheets [15]. In ATR-FTIR spectra the presence of phyllosilicates, *i.e.*, kaolinite and montmorillonite, is highlighted at the following wavenumbers: 3627 cm^{-1} ascribed to the inner hydroxyl groups, *i.e.*, those completely enclosed by aluminium and oxygen atoms; 1192 cm^{-1} (Fig. 3) assigned to the out-of-plane stretching Si-O-Si vibration; 1034 cm^{-1} due to the in-plane stretching Si-O-Si vibration, and 921 cm^{-1} (Fig. 3), 525 and 452 cm^{-1} associated with the bending vibrations of Al-Al-OH, Si-O-Al and Si-O-Si, respectively (Fig. 2) [16–20]. Also, in the ATR-FTIR spectra of samples there are two absorption bands of very weak intensities, *i.e.* 3392 cm^{-1} and 1634 cm^{-1}, which are attributed to the stretching and bending OH vibrations of water molecules present in the samples, especially in the montmorillonite mineral which has a high affinity to the water [15]. Regarding the presence of organic matter in the samples, we identified two very weak and sharp peaks at 2926 and 2852 cm^{-1} which are associated with asymmetric and symmetric stretching vibrations of CH_2 aliphatic group.

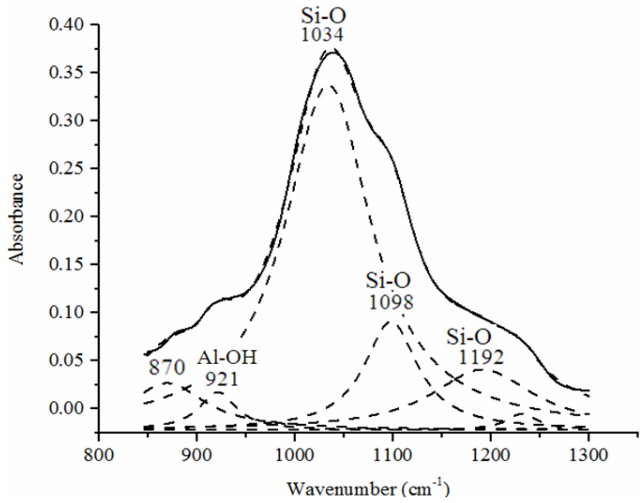

Fig. 3 – Deconvolution of complex IR absorption band comprised between 850 and 1300 cm^{-1}.

For CH_2 bending vibrations we found only a very weak absorption band at around 1456 cm^{-1} [5, 6], the other bands being superposed with the IR absorption bands of silicate groups. In addition, it is important to mention that the intensities of aliphatic methylene peaks are higher in the case of ATR-FTIR spectra of S_{1F-5F} samples than in the case of spectra of S_{1-5} samples (Fig. 2). For this reason, we may conclude that the S_{1F-5F} samples contain a greater concentration of organic carbon than the S_{1-5} samples. Consequently, ATR-FTIR technique proved to be a valuable tool to discriminate the biotic samples (S_{1F-5F}) from abiotic samples (S_{1-5}).

3.2. CHEMOMETRIC ANALYSIS

By the reduction of initial number of variables (1866 absorptions) to 234, in function of their Fisher's weight, we retained the most important wavenumbers which participated to the discrimination of B samples from the A samples. Analyzing the selected wavenumbers (Fig. 4) we remarked that they appear in three spectral regions *i.e.* 3100–2700 cm^{-1}, 1730–1600 cm^{-1} and 1500–1400 cm^{-1}, which contain IR absorption bands specific to the organic matter. Thus, the first and third spectral domains contain IR absorption peaks associated with stretching and bending vibrations of CH_2 group, respectively. In the second spectral domain there is an absorption band attributed to the bending OH vibrations of water molecules present in the samples (Figs. 2 and 4). Consequently, the characteristic IR absorption bands of organic matter have the best discrimination power of the fossil leaf samples (class B) from the sediment samples (class A).

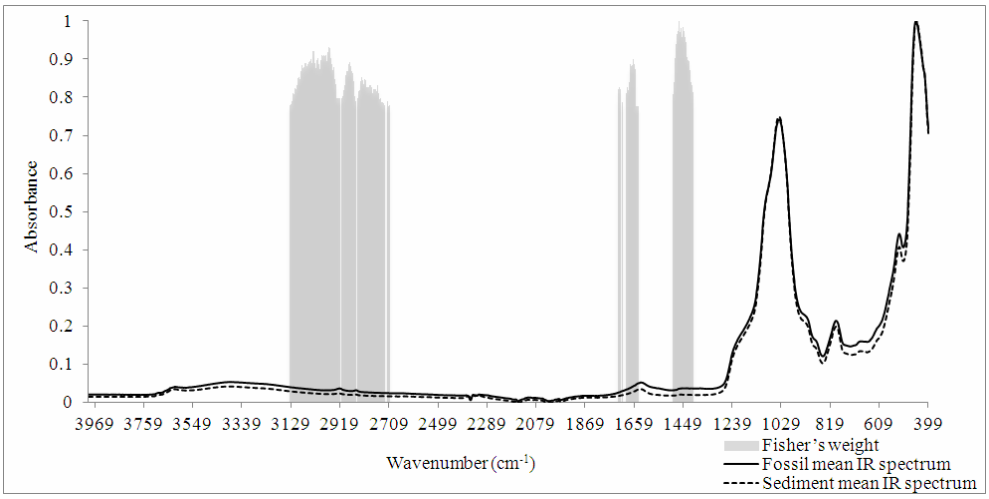

Fig. 4 – The mean ATR-FTIR spectra of fossil leaves and sediment samples and the first 234 important wavenumbers.

The dendrogram obtained by CA technique (Fig. 5) reveals us that the samples are clearly grouped into two clusters, S_1, S_4, S_2, S_3 and S_5 (class A) and S_{1F}, S_{3F}, S_{4F} and S_{5F} (class B), excepting the S_{2F} sample which is at the boundary between these two clusters. This result is confirmed by PCA technique. Thus, by plotting the first principal component *versus* the second principal component we can see that the samples are clustered, namely the B samples are grouped in the positive region of PC1, excepting the S_{2F} sample, while the A samples are in the negative region of PC1 (Fig. 6). Therefore, the first principal component, which has the highest explained variance (98.92%), is responsible with the discrimination of B-type samples from A-type ones.

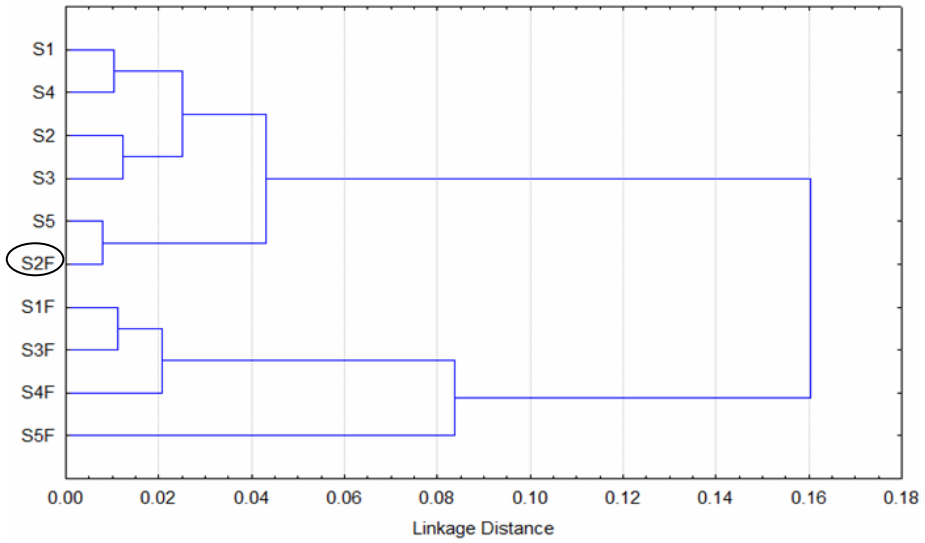

Fig. 5 – Dendrogram of the studied samples using the ATR-FTIR spectra.

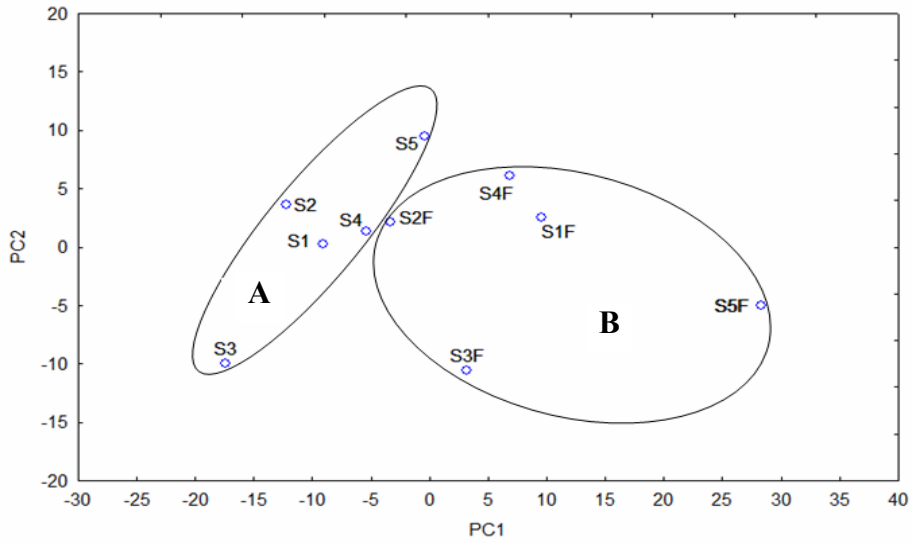

Fig. 6 – Plot of the PC1 score as a function of PC2 score.

3.3. X-RAY DIFFRACTION ANALYSIS

The XRD peaks (Fig. 7) indicate the presence of quartz, kaolinite and montmorillonite in all samples, the montmorillonite being in the highest percentage by weight, *i.e.*, between 61.8 wt% and 83.3 wt%, followed by the kaolinite – with a

percentage in the (11.3–30.4) wt% range – and the quartz, in the (5.1–11) wt% range (Table 1).

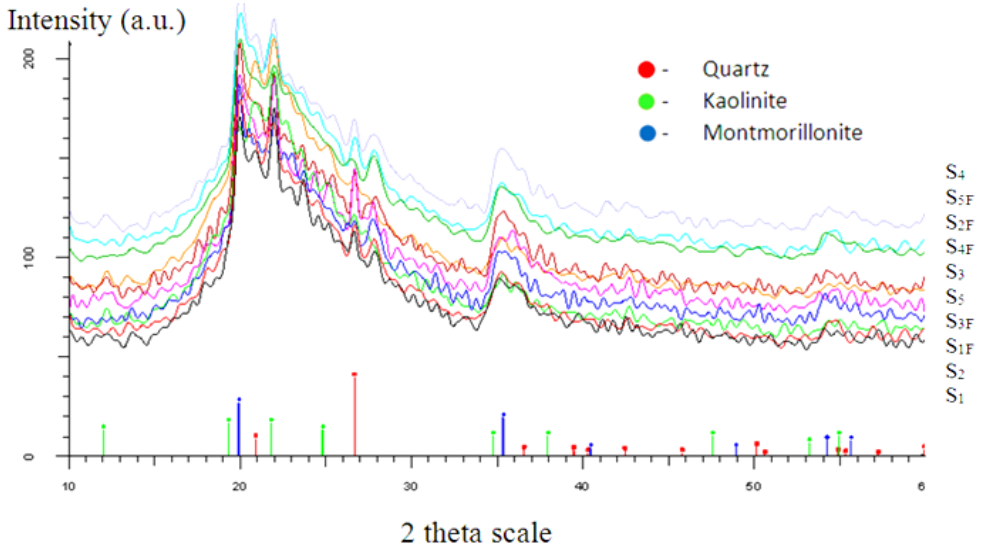

Fig. 7 – (Color online) XRD patterns of S_1 – S_5 and S_{1F} – S_{5F} samples. The spectra are assigned to the samples starting from bottom to top, in the order: S1, S2, S1F, S3F, S5, S3, S4F, S2F, S5F and S4.

Table 1

Mineral composition of samples (wt%)

Sample	Quartz	Kaolinite	Montmorillonite
S1	11.0	27.2	61.8
S1F	7.8	21.8	70.4
S2	6.3	20.7	73.0
S2F	5.1	16.5	78.4
S3	7.4	30.4	62.2
S3F	5.9	25.5	68.6
S4	8.6	16.3	75.1
S4F	7.3	14.5	78.2
S5	6.6	17.9	75.5
S5F	5.4	11.3	83.3

The elemental composition of studied samples is shown in Table 2. The chemical elements present in the samples are the following: H, O, Na, Mg, Al, Si, Ca and C. It is worth emphasizing the fact that the values of percentage by weight are almost the same or with small differences for all samples in the case of H, Na, Mg, Al and Si chemical elements while for O, Ca and C there are differences between percentages for the B and A samples.

Table 2

Elemental composition of samples (wt%)

Sample	H	O	Na	Mg	Al	Si	Ca	C
S1	0.6	42.9	0.8	5.5	7.2	30.7	10.3	4.3
S1F	0.8	33.1	0.7	4.7	7.4	32.3	17.2	7.5
S2	0.7	42.9	0.7	5.2	7.5	31.7	10.3	3.4
S2F	0.8	33.1	0.6	4.4	7.3	32.6	16.1	7.2
S3	0.9	43.6	0.5	3.2	7.3	33.8	10.4	4.3
S3F	0.8	34.1	0.7	4.7	7.4	35.3	13.2	7.3
S4	0.7	42.9	0.7	5.0	7.2	32.3	10.3	4.9
S4F	0.7	32.9	0.7	5.2	7.5	31.7	14.3	7.2
S5	0.7	42.9	0.7	5.0	7.4	32.0	10.2	4.2
S5F	0.9	33.6	0.5	3.2	7.5	33.8	15.4	6.8

Thus, we can see that the values of percentages are higher in the case of fossil leaf samples (B) than those obtained in the case of sedimentary rock samples (A) for the calcium and carbon elements. An inverse situation is encountered in the case of oxygen element, where the values of percentages are lower for B samples than for A samples.

4. CONCLUSIONS

The results of the present study revealed the fact that the ATR-FTIR spectroscopy was a sensitive and powerful technique for the mineralogical characterization of sedimentary rocks and fossil plants. More exactly, the analyzed samples in this paper contain three types of minerals, namely: quartz, kaolinite, montmorillonite. Also, the ATR-FTIR spectra clearly highlighted the presence of organic matter in the samples. The organic carbon, derived from the decomposition of plants, was identified by the presence of two sharp absorption peaks at 2926 and 2852 cm^{-1} which had a higher intensity for the fossil leaf samples than for the sediment samples. In this paper we also demonstrated that the ATR-FTIR spectra combined with the CA and PCA chemometric methods could discriminate the fossil leaf samples from the sediment samples, the characteristic IR absorption bands of organic matter having the best discrimination power.

Regarding the mineral composition of samples, the X-ray diffractograms provided the same results as those obtained from ATR-FTIR spectra regarding the samples main components – quartz, kaolinite and montmorillonite. A supplementary information given by the XRD technique is that the montmorillonite represents the main mineral from the samples, the percentage by weight being between 61.8 wt% and 83.3 wt%. Also, important information resulted from the XRD analysis of elemental composition of samples was that the main chemical elements present in the samples were oxygen, silicon and calcium. Another chemical element presents

in the samples was the carbon. It is important to mention that the values of carbon percentages were greater in the case of fossil leaves samples than those in the case of sedimentary rocks samples. This result is in agreement with that obtained from the ATR-FTIR spectra.

This study is the first performed in Romania and the proposed methodology could be useful for the detection and characterization of organic matter preserved in ancient sedimentary rocks in different fossiliferous complexes.

REFERENCES

1. G. Macovei, R. Givulescu, Carpth. J. Earth Environ. Sci. **1**, 1, 41–52 (2006).
2. M. Balachandran, Am. J. of Anal. Chem. **5**, 367–372 (2014).
3. Y. Chen, C. Zou, M. Mastalerz, S. Hu, C. Gasaway, X. Tao, Int. J. Mol. Sci. **16**, 30223–30250 (2015).
4. M. Ritz, L. Vaculíková, E. Plevová, D. Matýsek, J. Mališ, Clays and Clay Minerals **60**, 6, 655–665 (2012).
5. A. Guido, A. Mastandrea, F. Tosti, F. Demasi, A. Blanco, M. D'Elia, Memorie della Societa Astronomica Italiana Supplement, **20**, 64–68 (2012).
6. J.A. Heredia-Guerrero, J.J. Benítez, E. Domínguez, I.S. Bayer, R. Cingolani, A. Athanassiou, A. Heredia, Spectroscopy Europe, **28**, 2, 10–13 (2016).
7. L. Barbes, C. Radulescu, C. Stihi, Rom. Rep. Phys., **66**, 3, 765–777 (2014).
8. S. Gosav, A. Ene, R. Dragomir, Annals Dunarea de Jos Univ. Galati, Fasc. II. Mathematics, Physics, Theoretical Mechanics **8(39)**, 2, 242–247 (2016).
9. O.M. Cortea, R. Cristache, I. Sandu, Rom. Rep. Phys. **68**, 2, 615–622 (2016).
10. I. Călina, M. Demeter, E. Bădiţă, E. Stancu, A. Scărişoreanu, C. Vancea, Rom. Rep. Phys. **69**, 504 (2017).
11. I.B. Cozar, A.Pîrnău, L. Szabo, N. Vedeanu, C. Năstasă, O. Cozar, Rom. Journ. Phys. **61**, 7–8, 1265–1275 (2016).
12. S. Gosav, N. Paduraru, D. Maftei, M.L. Birsa, M. Praisler, Spectrochimica Acta Part A: Molecular and Biomolecular Spectroscopy **172**, 115–125 (2017).
13. M. Ritz, L. Vaculíková, E. Plevová, Acta Geodyn. Geomater. **8**, 1, 47–58 (2011).
14. S. Gosav, M.L. Birsa, Rom. Rep. Phys. **66**, 2, 411–426 (2014).
15. 15 R.A Schoonheydt, C.T. Johnston, *Surface and interface chemistry of clay minerals*. In: Bergaya, F., Theng, B.G.K., Lagaly, G. (Eds.), *Handbook of Clay Science*. Elsevier, Amsterdam, 87–112, 2006.
16. B.J. Saikia, G. Parthasarathy, J. Mod. Phys. **1**, 206–210 (2010).
17. R.T. Cygan, K. Tazaki, Elements **10**, 195–200 (2014).
18. B. Tyagi, C.D. Chudasama, R.V. Jasra, Spectrochimica Acta Part A **64**, 273–278 (2006).
19. J. Madejova, H. Palkova, M. Pentrak, P. Komadel, Clays and Clay Minerals **57**, 3, 392–403 (2009).
20. U.O Aroke, A. Abdulkarim, R.O. Agubunka, ATBU J. Environ. Tech. **6**, 1, 42–53 (2013).